

Automatic identification of glomerulus in the antenna lobe of *Drosophila Melanogaster*

Li Liu (stflily@stanford.edu)
Liang Liang (liangl@stanford.edu)
Project for CS229.
Dec 11, 09.

Abstract

Antenna lobe (AL) in the *Drosophila* brain is composed of ~50 glomeruli. Each of the glomeruli has a stereotyped shape, position, and neuronal composition. However, manually identification of the glomeruli usually is very time consuming and demands high familiarity with the structure. In this project, we applied Principle Component Analysis method via Singular Value Decomposition to identify a single glomerulus in AL. 105 training examples were used to construct the eigen basis for the AL image. Based on the coefficient of constructing AL eigen basis, the eigen basis for the target glomerulus images in the training set was also calculated. To identify the target glomerulus in the test examples, its AL image information was used as the input. The test results from the about 40 examples showed reasonably good reliability and robustness of the algorithm. Although we only trained the algorithm to identify a certain glomerulus (V glomerulus) in this case, this approach should also be applicable to other glomeruli so that many glomeruli in the AL can be recognized automatically.

1. Introduction

1.1 Antenna lobe and glomeruli

AL is the primary odor processing center in the model organism *Drosophila Melanogaster* (fruit fly). Over the last decade, biological research on neurons in AL has provided many insights on the development, organization, and information processing of the neural circuit [1-4]. AL has a very clear and stereotyped anatomy. One AL is composed of about 50 glomeruli, compactly packed into a 3D structure. Each glomerulus has its specific shape and localization in AL [5, 6] (Fig.1). Usually, a certain AL olfactory neuron innervates a single or a certain combination of glomeruli. By identifying the innervated glomeruli, the neuronal identity can be assigned. Thus in many studies on these neurons, an important step is to identify the glomeruli. This is usually accomplished by carefully comparing the morphology with a reference (like Fig 1b) and requires a lot of experience and time from the researcher. It would thus be very useful to develop an automatic method to reliably identify the glomeruli in AL.

1.2. Motivation and Principles

We propose to address the problem by first training an algorithm to recognize one of glomerulus. Then similar approach can be applied to the identification of other glomeruli one by one. In the end, given an AL image, a tagged AL like that in Fig. 1b can be automatically generated. To achieve one-glomerulus identification, we can take advantage of the neuronal organization in the AL. There are ~60 classes of odorant sensory neurons (OSN) in the fly. OSN project their axons into the AL and each class of OSN converge their axonal terminals into a single glomerulus. There are genetic methods available to label each class of the OSN. By labeling a single class of OSN, the corresponding glomerulus is labeled as well. This biological approach can be utilized to train the computer where the target glomerulus is localized. On the other hand, the whole AL morphology, as well as other neuropil, can be immunostained with specific synaptic markers independently from the ORN labeling. We will use the image from samples with both AL and

target glomerulus labeled to train the algorithm and then when a new image with only AL is introduced, the glomeruli identity will be assigned to it.

To develop the algorithm, we started from some intuitive methods based on our observation of the AL and target glomerulus. But these methods may lack the generality to other glomerulus and we thought a general machine learning method might be more robust. Specifically, we figured that the glomeruli identification is somehow similar to the face recognition problem and we might borrow some principles from the latter one.

Principle Component Analysis (PCA) is a widely used method for face recognition. In PCA, a set of ‘eigenfaces’ are first abstracted from the training data. Through the projection operation, a face image can be calculated as a weighted sum of the eigenfaces. By comparing these weights to those of known individuals, a new face can be recognized [7]. Eigenfaces with large singular values represent the more general features of the given faces, while those corresponding to relatively small singular values feature the variation among the faces. The eigenfaces with really tiny singular values can be to some extent treated as the unexpected distortion in the training data.

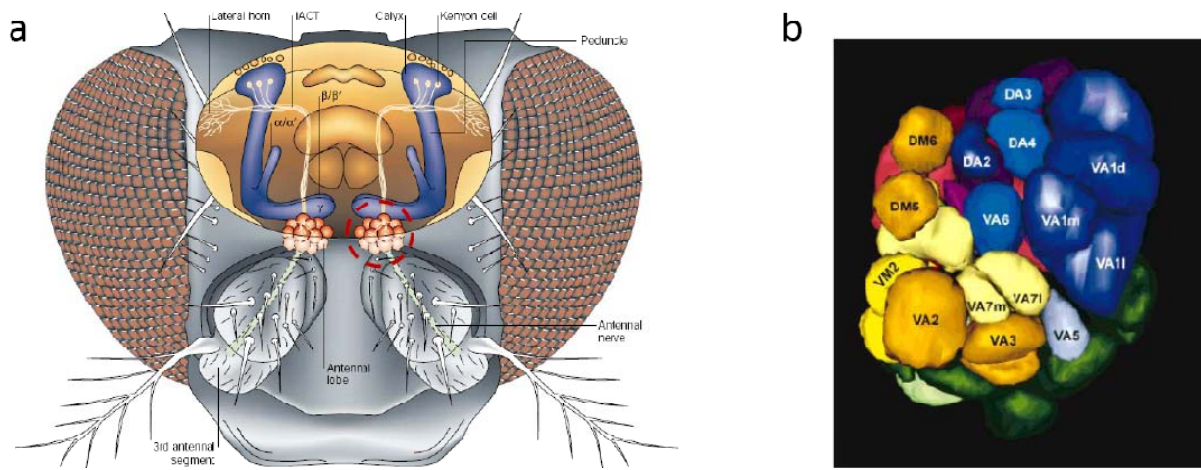


Figure 1. Anatomy for a fly brain and a AL. **a.** Scheme of the anatomy of a fly brain. An AL was circled out. **b.** A more detailed scheme for the circled AL as shown in A. The AL as seen from the anterior. Lateral is to the right, dorsal on top. 15 glomeruli are named in this figure [5, 8].

In the case of glomeruli identification, we took advantage of the correlation between the two intensity matrices in the same example (AL matrix--labeling mostly AL and some other brain regions, and target glomerulus matrix--only highlighting the glomerulus we are trying to identify), and correlated their ‘eigenfaces’. Specifically, the AL matrices were used to calculate the eigen basis for the AL feature space. Technically, each AL eigen basis can be represented as the weighted sum of the training AL vectors. The same weights were then used to calculate the corresponding eigen basis for the target glomerulus feature space. When a new AL image was given, it was projected to the AL eigen basis and the coefficients of the projection was treated as the weights to sum up the target glomerulus eigen basis and thus construct the target glomerulus for the new AL image. The location of the constructed glomerulus in the new AL image therefore was assigned the identity of the target glomerulus.

Moreover, we tried to avoid possible local distortions in the images and to predict the location of

the glomerulus in its most reasonably possible place. We figured data compression (reduce the matrix dimension) could mitigate those undesired intensity fluctuations. Besides, we also dropped the singular vectors with tiny singular values when we constructed the basis. This improved the recognition result and lowered the computation complexity. In addition, the images were scanned with roughly good alignment from symmetry intuition of the experimenter, which dramatically reduces the dimension of basic space and allows the use of techniques similar to face recognition for glomeruli identification.

2. Methods and Results

2.1 AL and target glomerulus images

The AL and target glomerulus (V glomerulus, labeled with Gr21a-Gal4, UAS-RFP) images in the training and test set were obtained by confocal laser scanning microscope in Liqun Luo lab at Dept of Biology in Stanford University. For each fly sample, the whole brain was dissected out and immunostained against the presynaptic marker nc82 (labeling neuropil and thus revealing AL as well as other brain region structures) and the RFP (labeling the target glomerulus). The secondary antibodies are conjugated with different fluorophores so that the neuropil and target glomerulus can be spectrally separated--the neuropil (AL regions) was in the purple channel whereas the target glomerulus was scanned in the red channel as shown in Fig 2. Since the AL is about $50\mu\text{m}\times 50\mu\text{m}\times 50\mu\text{m}$, 40~50 single plane images were taken (with 1 μm step in between) to go through the whole depth of AL. At each single z plane, a 512 pixel \times 512 pixel scanning was performed at a resolution of 4.8 pixels/ μm . The zoom in the x-y dimension was slightly adjusted from sample to sample so that the scanned ALs were about similar sizes laterally. An example scanned sample is shown in Fig 2. The target glomerulus usually spans 2/5 of the entire z stack.

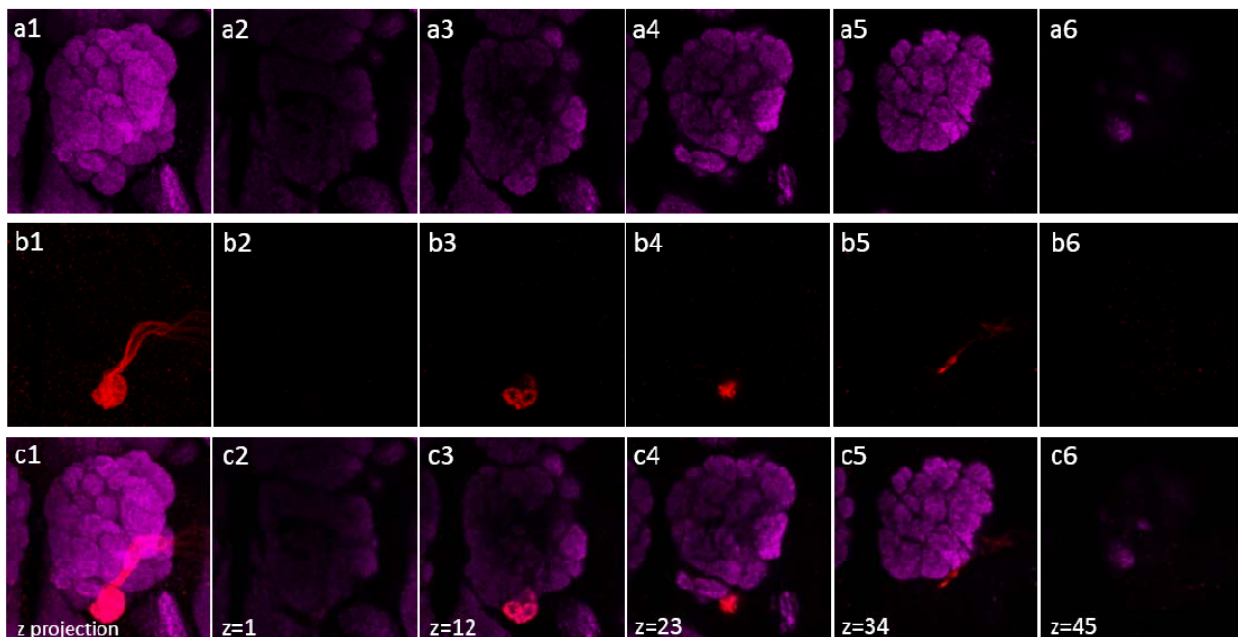


Figure 2 AL and target glomerulus images from a sample. **a.** The AL images. **b.** Target glomerulus images. **c.** Overlay of the AL and target glomerulus images. *1, the maximum projection of the whole z stack (z total is 46); *2, *3, *4, *5, *6, single z plane image from z=1, z=12, z=23, z=34, z=45, respectively. *=a, b, c. AL is labeled in purple. Target glomerulus is labeled in red.

2.2 Data processing

Each sample image usually contains 40~50 z planes. Each z plane (denoted as an example) has two separate channels, one for AL and one for the target glomerulus. The training set is a collection of 105 single z plane images (examples) from 5 AL samples, with 21 examples per sample, usually the middle ones of the z stack. We didn't choose exactly the same z planes cross samples, since the samples had different sizes and occupied different depth, and there was no standard reference points at which to start and end the z stack during image acquisition--just roughly from the emergence to the disappearance of the AL. Each example was read by MATLAB as a $512 \times 512 \times 2$ matrix, where 512 is the number of pixels in x/y dimension and 2 refers to the two sets of matrices (AL and the target glomerulus).

The scanned images usually contained noises (due to the nonspecific immunostaining) and had regions outside AL labeled. We manually removed those images either with too much noise or at undesired z plane (with a lot of other brain regions) beforehand, which comprised about 15% of the total collected data.

Another step we took at this stage was data compression, to reduce random noises (due to shot noise and dark noise) and to reduce the data dimension. By reducing the dimension from 512×512 to 64×64 , the processing time dropped from 20 ~ 25 minutes to a few seconds, with not much influence on the target glomerulus identifying accuracy. But 64×64 was not mandatory, and we actually worked on images at both 256×256 and 64×64 resolutions.

2.3 Eigen Basis Construction

The 512×512 intensity matrix for each channel in a given example was reshaped into a 262144 ($=512 \times 512$) dimension vector. A 262144×105 AL training matrix $M=[m_1, m_2, \dots, m_{105}]$ was thus formed where each column represented one AL training image. Similarly, $N=[n_1, n_2, \dots, n_{105}]$ was used to denote the training matrix of the target glomerulus. The mean value of m_1, m_2, \dots, m_{105} (m_{mean}) was then subtracted from m_1, m_2, \dots, m_{105} to form $M^*=[m_1^*, m_2^*, \dots, m_{105}^*]$. The AL image of m_{mean} is shown in figure 3.



Figure3. The mean of 64×64 AL images in the training set. Note: AL is artificially labeled in red instead of purple for the convenience of displaying images.

In order to centralize the final decision of the position of the targeted glomerulus, we also pre-eliminated all the points whose intensities were smaller than a particular threshold in the glomerulus -- by setting the corresponding matrix element to zero. In our particular example, we set the threshold to be 20% of the maximum intensity value in each column.

The left singular vectors of M^* formed the eigen vectors of the whole AL image space. Due to the extremely high dimensions, it was impractical to do singular value decomposition in MATLAB directly. A viable approach was to find the left singular vectors from their

corresponding right singular vectors whereas the right singular vectors were eigenvectors of $M^{*T}M^*$, a 105×105 matrix.

The formula to transform from right unitary singular vectors to left unitary singular vectors is given by $u_i = M^*v_i / \sqrt{d_i}$, where d_i is the non-zero i th eigenvalue of $M^{*T}M^*$, v_i is the i th unitary eigenvector of $M^{*T}M^*$ or the i th right unitary singular vector of M^* , and u_i is the i th left singular value.

Singular vectors corresponding to the singular values smaller than a certain threshold were dropped. Since we had about 100 training examples in this case, we set the threshold to be 0.0003 of the largest singular value. The eigen basis space we obtained in the end was composed of about 64 eigenvectors. The first 4 AL eigen images were shown in the red channel in Fig 4.

2.4 Identify the target glomerulus in each of the eigen basis vectors

The eigen basis for the target glomerulus was calculated based on the principle discussed in section 1.2. The eigen basis for AL matrix was first obtained. Each eigen basis can be considered as an linear combination of all the example AL vectors (the column vector of M^*)—to calculate u_i , for example, the coefficients were actually the corresponding elements in v_i . The same coefficient for the linear combination was used to form the eigen basis for the target glomerulus matrix. Mathematically, the matrices corresponding to the AL and target glomerulus are $M^* = [m_1^*, m_2^*, \dots, m_{105}^*]$ and $N^* = [n_1^*, n_2^*, \dots, n_{105}^*]$. $\{u_1, u_2, \dots, u_k\}$ ($k = 64$ in our case) form the eigen basis of the AL image space, and $u_i = \sum_{j=1}^{105} a_{ij}m_j$, then $w_i = \sum_{j=1}^{105} a_{ij}n_j$ gives the i th eigen basis vector for the target glomerulus image space. The plot of the first 4 eigen basis with the corresponding glomerulus labels are shown in the green channel in Fig 4 (from 512×512 and 64×64 respectively for comparison).

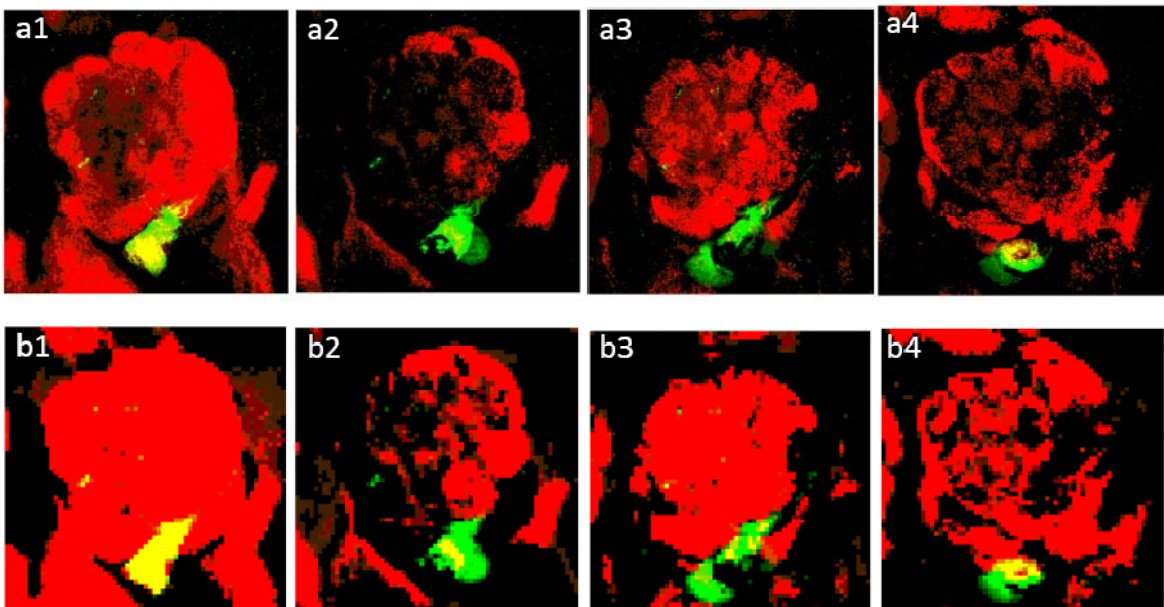


Figure 4. The first 4 calculated eigen images at 512×512 and 64×64 resolutions. a. Eigen images at 512×512 resolution. b. Eigen images at 64×64 resolution. Red: AL channel. Green: target glomerulus channel. Yellow: overlay.

To get an idea about the singular vectors corresponding to relatively small singular values we also plotted the 70th and 80th singular vector in Fig 5. In these plots, the intensity was relatively

uniformly distributed and didn't even fit into the preliminary shape of AL. It confirmed our speculations that they rather carried the noise information. Another important aspect worth noticing was that we almost couldn't see any target glomerulus labeling there, which also validated our decision to drop these singular vectors corresponding to really small singular values.

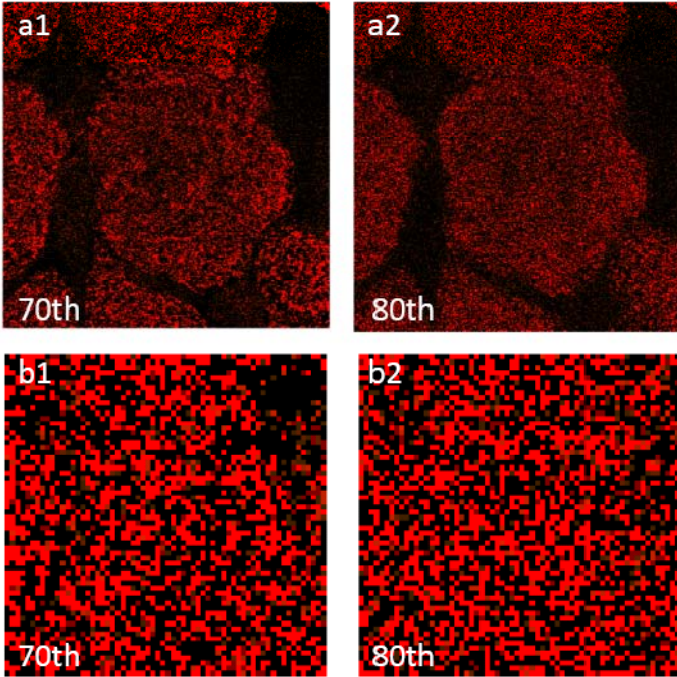


Figure 5. The 70th and 80th eigen images at 512x512 (a) and 64x64 resolution. Red: AL channel. Green: target glomerulus channel. Yellow: overlay.

2.5 Test principle and result

The 60 test examples were collected under the same imaging conditions, and selected from the same criteria regarding to the z plane, noise level and image distortion. The same preprocessing steps were carried on these test examples. We also made sure that none of the test examples were taken from samples used in the training set.

To identify the position of target glomerulus in the test examples, our strategy was to construct the target glomerulus based on the AL image in the same example set. To achieve that, we first projected the AL matrix of the test example onto the AL eigen basis vectors $\{u_1, u_2, \dots, u_{k=64}\}$ as was usually done in the face recognition process. Then the same set of projection coefficients were used to calculate the weighted combination of the target glomerulus eigen basis vectors $\{w_1, w_2, \dots, w_{k=64}\}$. Mathematically, $n_{\text{test}}^* = \sum_{j=1}^k b_j w_j$, where $b_j = (m_{\text{test}}^*)^T u_j$, and u_j, w_j are the eigenbasis for the AL matrix and target glomerulus matrix. Randomly chosen results are shown in Fig 6. We can see that the algorithm can predict pretty well the location of the target glomerulus when the test AL image is close to the mean of training AL image (Fig 6 b1,b2). When the test AL image is far off the mean of training AL image, the predicted target glomerulus is roughly around the true region.

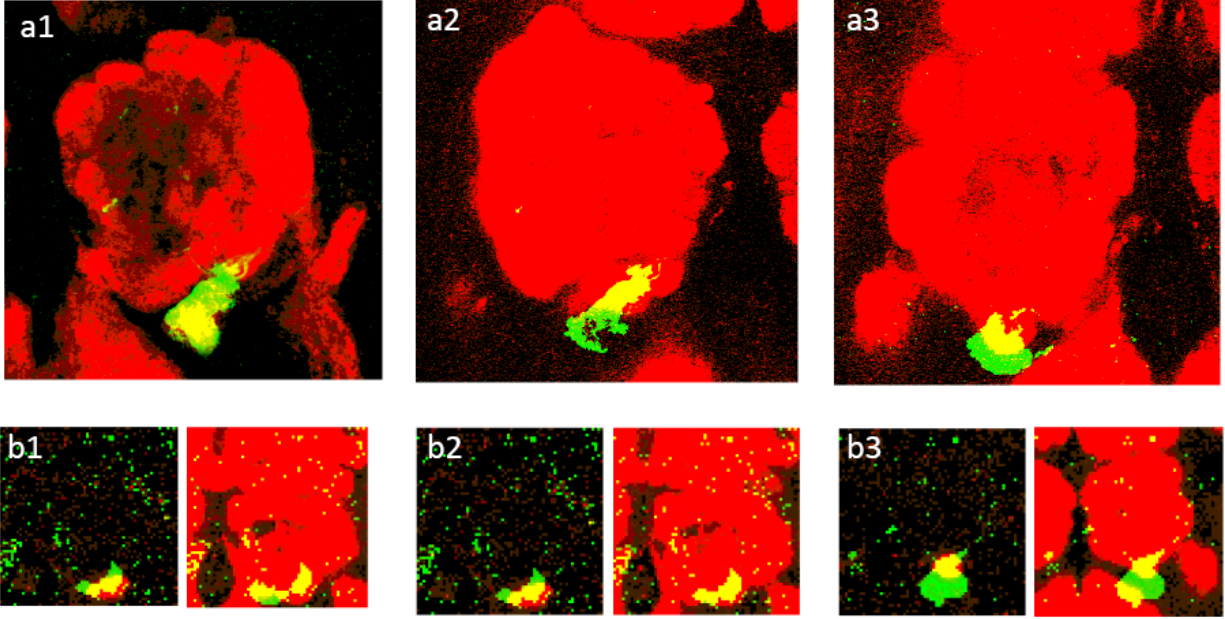


Figure 6. The test result of predicting target glomerulus position at 512x512 and 64x64 resolutions. **a.** Three samples of the predicted target glomerulus position at 512x512 resolution. Red: test AL image; Green: predicted target glomerulus; Yellow: Overlay. **b.** Three samples of the predicted target glomerulus position at 64x64 resolution. For each b_i , the image on the left is the overlay between the real target glomerulus (red) and the predicted target glomerulus (green), the image on the right is the overlay between the AL (red) and the predicted target glomerulus (green).

3. Discussions and Future Work

The approach we applied to identify the glomerulus in our project mainly originated from the PCA face recognition algorithm. Although the estimation on the position of the target glomerulus was quite satisfactory, our method didn't fully utilize the information contained in both the training and test data, or capture the unique properties of this specific problem. Both the training and test data describe dynamic process (data went through a series of z planes) and a close observation showed that there was actually a close relationship between the intensity change of the elements for the target glomerulus and non-target glomerulus parts over the Z_s . Plots of the intensity change of the glomerulus randomly chosen from the training example in contrast with the non-target intensity change are shown in Fig 7.

The plots of intensity change shows that the intensity for the target glomerulus is more concentrated on the left side (corresponding to smaller z numbers). Their intensity is also less spread and generally has only one peak. On the other hand, the intensity of non-glomeruli elements are more sparsely distributed and could have multiple peaks. Those differences could be mathematically captured with $\bar{x} = \sum_{i=1}^{40} x_i y_i / \sum_{i=1}^{40} y_i$, $\overline{\text{var}} = \sum_{i=1}^{40} (x_i - \bar{x})^2 y_i / \sum_{i=1}^{40} y_i$.

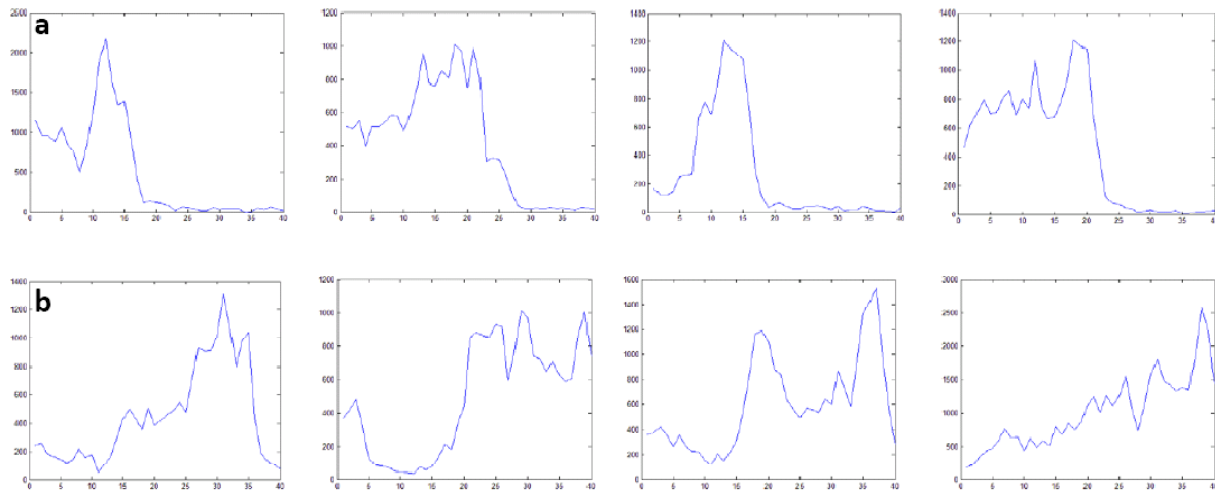


Figure 7. The intensity change with depth. a. The intensity change of the glomerulus region over depth from four samples. b. The intensity change of the non-glomerulus region over depth from four samples. The y-axis is the intensity, and the x axis is the depth (number of the z plane).

However full dependence on those features, as we tried, was not an optimal choice. The test error from the true value was more obvious. Our next step is to try to combine these two approaches to see if we could get better results.

4. References

1. Olsen, S.R. and R.I. Wilson, *Lateral presynaptic inhibition mediates gain control in an olfactory circuit.* Nature, 2008. **452**(7190): p. 956-60.
2. Wang, J.W., et al., *Two-photon calcium imaging reveals an odor-evoked map of activity in the fly brain.* Cell, 2003. **112**(2): p. 271-82.
3. Vosshall, L.B. and R.F. Stocker, *Molecular architecture of smell and taste in Drosophila.* Annu Rev Neurosci, 2007. **30**: p. 505-33.
4. Komiyama, T., et al., *Graded expression of semaphorin-1a cell-autonomously directs dendritic targeting of olfactory projection neurons.* Cell, 2007. **128**(2): p. 399-410.
5. Laissue, P.P., et al., *Three-dimensional reconstruction of the antennal lobe in Drosophila melanogaster.* J Comp Neurol, 1999. **405**(4): p. 543-52.
6. Couto, A., M. Alenius, and B.J. Dickson, *Molecular, anatomical, and functional organization of the Drosophila olfactory system.* Curr Biol, 2005. **15**(17): p. 1535-47.
7. Turk, M. and A. Pentland, *Eigenfaces for Recognition.* Journal of Cognitive Neuroscience, 1991. **3**(1): p. 71-86.
8. Heisenberg, M., *Mushroom body memoir: from maps to models.* Nat Rev Neurosci, 2003. **4**(4): p. 266-75.